Cell

Selective Evolution of Stromal Mesenchyme with p53 Loss in Response to Epithelial Tumorigenesis

Reginald Hill,[1] Yurong Song,[2] Robert D. Cardiff,[3] and Terry Van Dyke[2,*]
[1] Curriculum in Genetics and Molecular Biology
[2] Department of Genetics
University of North Carolina at Chapel Hill, Chapel Hill, NC 27599, USA
[3] Center for Comparative Medicine, University of California at Davis, Davis, CA 95616, USA
*Contact: tvdlab@med.unc.edu
DOI 10.1016/j.cell.2005.09.030

SUMMARY

Our understanding of cancer has largely come from the analysis of aberrations within the tumor cell population. Yet it is increasingly clear that the tumor microenvironment can significantly influence tumorigenesis. For example, the mesenchyme can support the growth of tumorigenic epithelium. However, whether fibroblasts are subject to genetic/epigenetic changes as a result of selective pressures conferred by oncogenic stress in the epithelium has not been experimentally assessed. Recent analyses of some human carcinomas have shown tumor-suppressor gene mutations within the stroma, suggesting that the interplay among multiple cell types can select for aberrations nonautonomously during tumor progression. We demonstrate that this indeed occurs in a mouse model of prostate cancer where epithelial cell cycle disruption via cell-specific inhibition of pRb function induces a paracrine p53 response that suppresses fibroblast proliferation in associated stroma. This interaction imposes strong selective pressure yielding a highly proliferative mesenchyme that has undergone p53 loss.

INTRODUCTION

Epithelial-mesenchymal interactions are critical in regulating many aspects of vertebrate embryo development, and studies have shown that input from the stroma is necessary not only for the development of many structures including the prostate (Cunha et al., 1996; Podlasek et al., 1999), mammary gland (Sakakura, 1991), and limb (Johnson and Tabin, 1997) but also for the maintenance of homeostatic equilibrium in adult tissues with the stromal cells maintaining control over cell size, function, and response to wounds and other pathological conditions (reviewed in Tlsty and Hein [2001]) through modification of the extracellular matrix (ECM). Recently, the uterine stroma has been shown to mediate both developmental and estrogen-mediated changes in the epithelium, a process involving Wnt5a (Mericskay et al., 2004). The interactions between epithelium and mesenchyme are believed to be mediated by paracrine signals and ECM components secreted from developing mesenchyme that affect adjacent epithelia (Cunha et al., 1980). In response to tumorigenesis in adjacent epithelial cells, fibroblasts, a major stromal component, also undergo changes that may alter the normal epithelial-mesenchymal interactions (Bergers and Coussens, 2000). Several experimental systems have further shown that such ''cancer-associated'' fibroblasts can enhance the tumorigenic properties of the epithelial compartment (Barcellos-Hoff and Ravani, 2000; Bhowmick et al., 2004b; Cunha et al., 2003; Ohuchida et al., 2004). However, whether the tumor mesenchyme undergoes selective genetic or epigenetic changes in specific loci in response to epithelial tumorigenesis and thus can coevolve has not been experimentally examined.

Recently, several labs have reported the mutation of the tumor-suppressor genes, including *p53*, in the stromal compartment of human carcinomas. *p53* is mutated in the most advanced forms of human cancers, comprising most tumor types (Levine et al., 1991; Nigro et al., 1989; Hollstein et al., 1991). In response to several stress signals, including oncogene activation, DNA damage, and physiological stress, p53 levels increase leading either to growth arrest or apoptosis (reviewed in Harris and Levine [2005]; Vousden and Lu, 2002). Because of its checkpoint roles, p53 inactivation can also contribute to tumorigenesis by propagation of genomic instability. The stimulation of angiogenesis has also been associated with p53 loss (Dameron et al., 1994; Yu et al., 1997). The factors that determine which response is elicited are not clearly understood, although cell type and

nature of the stress appear to have a role. Yet recent evidence showing p53 alterations in the stroma associated with carcinomas of many tissue types (Fukino et al., 2004; Kurose et al., 2001, 2002; Matsumoto et al., 2003; Moinfar et al., 2000; Paterson et al., 2003; Tuhkanen et al., 2004; Wernert et al., 2001), including the prostate (see Discussion), suggests non-cell-autonomous mechanisms for p53 induction could play a role in tumor suppression. Although oncogenic stress (the induction of tumorigeneic properties) has previously been shown to cell-autonomously induce p53 responses (Vousden, 2002), leading to selective pressure for p53 inactivation and tumor progression, whether cell nonautonomous induction of p53 may play a role in tumor evolution has not been explored.

Here, we uncover such a mechanism in the study of a genetically engineered spontaneous prostate cancer model. *TgAPT*$_{121}$ mice develop extensive prostatic intraepithelial neoplasia (mPIN) as a result of inactivating pRb and related proteins p107 and p130 specifically in prostate epithelium by probasin-driven expression of T_{121} (a 121 aa N-terminal fragment of SV40 large T antigen). T_{121} fully inactivates pRb function by eliminating the redundancy/compensation provided by p107 and/or p130 commonly observed in the mouse (Dannenberg et al., 2000; Lee et al., 1996; Luo et al., 1998; Robanus-Maandag et al., 1998; Sage et al., 2000; Xiao et al., 2002). We previously showed that T_{121}-induced mPIN results from extensive aberrant epithelial proliferation accompanied by Pten-dependent apoptosis. By 4 months, mPIN lesions progress to microinvasive adenocarcinoma in all animals, a process that is accelerated in a *Pten*$^{+/-}$ background (Hill et al., 2005). In an effort to determine the role, if any, for p53 in prostate cancer suppression, we examined the development of prostate lesions in *TgAPT*$_{121}$ mice with alterations in the *p53* genotype. Surprisingly, while epithelial apoptosis and proliferation is unaffected by p53 deficiency (Hill et al., 2005), a significant role for p53 in the mesenchyme was induced by the T_{121}-initiated epithelium. Here, we examine the impact of this paracrine-selective pressure on tumor evolution.

RESULTS

Increased Mesenchymal Response in *TgAPT*$_{121}$ Prostate upon p53 Deficiency

We assessed the role of p53 in prostate tumor suppression by examining the progression of tumors in *TgAPT*$_{121}$ mice that were wild-type, heterozygous, or null for *p53*. Prostates of wild-type mice consist of normal glandular architecture with a single luminal epithelial cell layer (Figure 1A, arrow) and an underlying basal cell layer separated from surrounding stroma (Figure 1A, arrowhead) by a basement membrane (Shappell et al., 2004; Figure 1A). As previously reported (Hill et al., 2005), *TgAPT*$_{121}$*;p53*$^{+/+}$ prostates, in which T_{121} is induced in the epithelium upon androgen induction at puberty, are extensively dysplastic by 2 months of age, with the epithelium characterized by nuclear atypia and loss of single-layer architecture (Figure 1B). In these mice, disease progression is reproducible and 100% penetrant, with widespread dysplasia becoming murine prostatic intraductal neoplasia (mPIN) and producing minimally invasive adenocarcinoma over time (Figure 1J; Hill et al., 2005). At early times (<3 months), *TgAPT*$_{121}$*;p53*$^{+/-}$ prostates were indistinguishable from those of *TgAPT*$_{121}$*;p53*$^{+/+}$ littermates (Figures 1C and 1K), while the *TgAPT*$_{121}$*;p53*$^{-/-}$ prostate epithelium was morphologically distinguishable in that nuclear atypia, including multinucleation, was more extensive with earlier onset (Figures 1D and 1L). Notably, subsequent to T_{121} expression in the epithelial compartment, p53-deficient *TgAPT*$_{121}$ prostates contained an extensive hypercellular mesenchyme (Figure 1E, star), consistent with a strong stromal response upon p53 inactivation in one or more compartments. Importantly, *p53*$^{-/-}$ prostates are morphologically normal (not shown). Thus, these effects, including the mesenchymal response, are dependent on expression of the T_{121} exclusively in the epithelium (Figure 1I; Hill et al., 2005).

Tumor Progression with Massive Stromal Involvement Facilitated in *p53* Heterozygous and Null *TgAPT*$_{121}$ Mice

Further evidence for a stromal p53 effect came from the analysis of tumor progression. In *TgAPT*$_{121}$*;p53*$^{+/-}$ mice, distinct tumors emerged focally from the anterior prostate at 5 months of age (Figure 1F, arrows, and Figure 1K) and grew rapidly, becoming massive by about 7 months (Figure 1K). In addition to the adenocarcinoma histopathology observed in *TgAPT*$_{121}$*;p53*$^{+/+}$ prostates (Figure 1J; Hill et al., 2005), these tumors had developed an extensive abnormal mesenchyme (Figure 1G, star), which expressed fibroblast markers smooth muscle α actin (SMA; Figure 2D) and fibroblast-specific protein marker S100A4 (FSP; Strutz et al., 1995; Figure 2E). Cytokeratin (CK) 8 expression remained confined to the luminal epithelial cells (Figure 2C), indicating a true effect in the stroma and not an active epithelial to mesenchymal transition (EMT; Figure 2; n = 9). For comparison, *TgAPT121;p53*$^{+/+}$ prostates at 12 weeks of age also show clear compartmental separation as verified by epithelial CK8 and mesenchymal SMA expression (Figures 2A and 2B, respectively).

Morphologically, the prominent *TgAPT*$_{121}$*;p53*$^{+/-}$ tumors could be classified as ''phylloides-like'' because of their resemblance to human breast and prostate phylloides tumors (Shappell et al., 2004). However, unlike the usually benign human tumors, these tumors reached massive size, growing very rapidly (from 0.5 cm^3 to > 2 cm^3 over 4 weeks), engulfing many of the organs of the urogenital system and filling the abdominal cavity. Given this difference, these tumors are herein referred to as ''stromal tumors,'' although the epithelium also comprises a significant abnormal component. Importantly, similar stromal tumors were also observed in 44% of male *TgAPT*$_{121}$*;p53*$^{+/+}$ mice, but only after 11 months of age (Figure 1J). Thus, development of such tumors was facilitated by *p53* heterozygosity but clearly required the *APT*$_{121}$ transgene, since transgene negative *p53* heterozygous prostates were fully normal (not shown). Furthermore, all *TgAPT*$_{121}$*;p53*$^{-/-}$ mice developed similar stromal tumors even more rapidly by 11 weeks of age (Figures 1H and 1L).

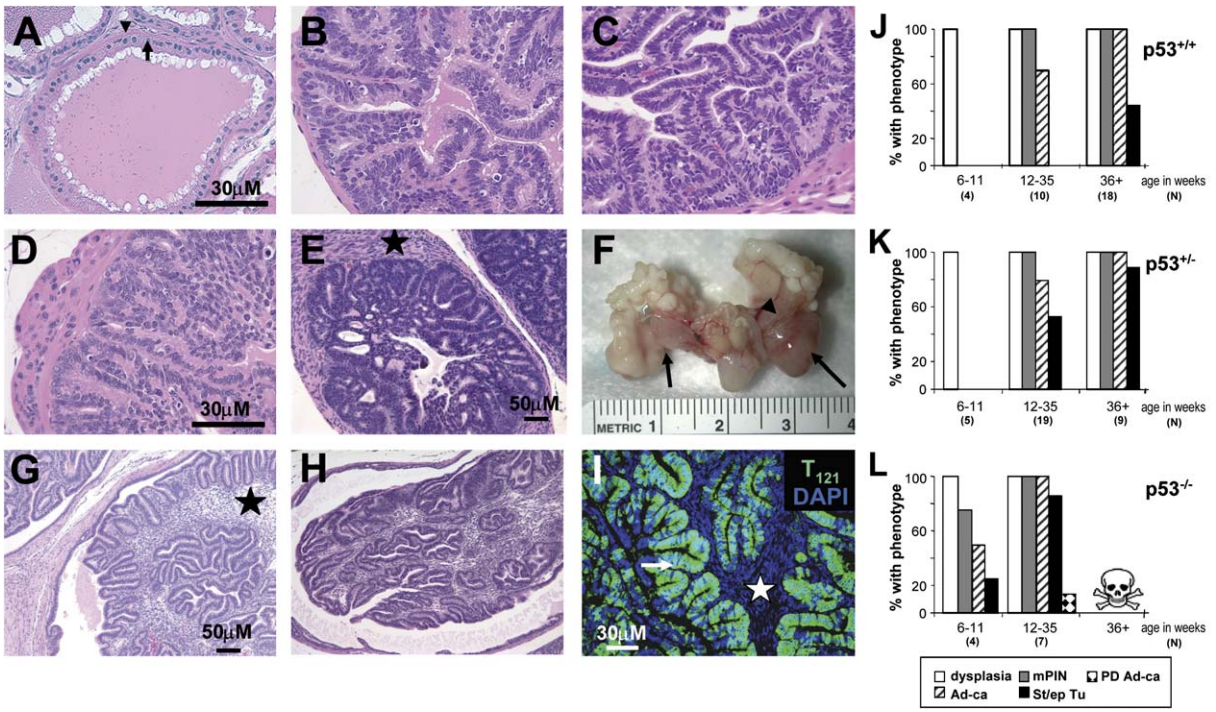

Figure 1. Histological Characterization and Temporal Progression of Prostate Tumorigenesis in *TgAPT$_{121}$* Prostates of Distinct *p53* Genotypes

Prostate morphologies in H&E-stained sections of 2-month-old mice are shown: (A) wild-type mice with a normally thin layer of epithelial (arrow) and stromal cells (arrowhead), (B) *TgAPT$_{121}$;p53$^{+/+}$*, (C) *TgAPT$_{121}$;p53$^{+/-}$*, and (D) *TgAPT$_{121}$;p53$^{-/-}$*. The epithelial cells in *TgAPT$_{121}$;p53$^{-/-}$* prostates are pleiotropic and grow in dense patterns. *TgAPT$_{121}$;p53$^{-/-}$* prostates contain an extensive hypercellular mesenchyme ([E], star). Stromal tumors develop in *TgAPT$_{121}$;p53$^{+/-}$* mice as young as 22 weeks of age (G) and consist of an abundance of stromal cells (star). These stromal tumors develop in *TgAPT$_{121}$;p53$^{-/-}$* mice by 11 weeks (H). Stromal tumors ([F], arrows) in a 5-month-old *TgAPT$_{121}$;p53$^{+/-}$* mouse prostate arose focally from the anterior prostate (arrowhead). In these tumors T_{121} is expressed in epithelial cells ([I], arrow) but not in the stroma (star) as detected by immunofluorescence. T_{121} is visualized as the merge (aqua) of green flourescein signal with blue DAPI counterstaining.

(J) By 8 weeks, *TgAPT$_{121}$* prostates broadly exhibit dysplasia, which is characterized by atypical cells with condensed chromatin, nuclear elongation, and epithelial layer tufting. By 12 weeks, mPIN is extensive and regions of adenocarcinoma (Ad-ca) are often detected, characterized by further deterioration of cellular morphology, disorganized growth patterns, and the presence of small back-to-back glands. Some mice develop stromal tumors (St/ep Tu) around 11 months.

(K) *p53* heterozygosity increases the frequency and accelerates the onset of stromal tumors while mPIN and Ad-ca develop similarly to *TgAPT$_{121}$* mice.

(L) *p53* nullizygosity accelerates the onset of mPIN, adenocarcinoma, and stromal tumors. *TgAPT$_{121}$;p53$^{-/-}$* mice also show the development of poorly differentiated tumors (PD Ad-ca) at 22 weeks of age. Due to tumor-burden limitations, *TgAPT$_{121}$;p53$^{-/-}$* mice could not be aged beyond 24 weeks. The number of animals analyzed in each group is indicated in parentheses.

p53 Deficiency Results in Increased Mesenchymal Cell Proliferation

Since the stroma was significantly expanded in *TgAPT$_{121}$;p53$^{-/-}$* prostates early in life with early onset of stromal tumors and similar tumor development increased in frequency and was accelerated in a *p53$^{+/-}$* relative to *p53$^{+/+}$* background, we hypothesized that initiating tumorigenesis in the epithelium by inactivation of pRb function had non-cell-autonomously elicited a p53-mediated response in the stromal fibroblasts resulting in the suppression of their proliferation. Thus, reduction or loss of p53 in one or both compartments facilitated fibroblast proliferation and tumor development. To test this hypothesis, we first examined the levels of cell proliferation and p53 expression in epithelial and stromal compartments prior to and after stromal tumor development in each background. Using Ki67 immunofluoresence (IF) to detect S phase cells, we confirmed that epithelial cells in all cases showed similar high levels of proliferation as previously determined (Figure 3; Hill et al., 2005). At 2 months of age, soon after transgene induction in prostate epithelium, *TgAPT$_{121}$;p53$^{+/+}$* and *TgAPT$_{121}$;p53$^{+/-}$* prostatic mesenchyme rarely contained Ki67-positive cells (Figures 3A, 3B, and 3E). However, proliferating cells were readily detected by this age within *TgAPT$_{121}$;p53$^{-/-}$* mesenchyme (Figures 3C and 3E). In all *TgAPT$_{121}$* backgrounds, once stromal tumor masses were detectable, fibroblast proliferation was widespread (Figure 3D), with Ki67-positive cells comprising about 50% of that population (Figure 3E).

p53 Expression Loss in Stromal Tumor Fibroblasts

To further define the relationship between p53 and the emergence of abnormal mesenchyme, we examined p53

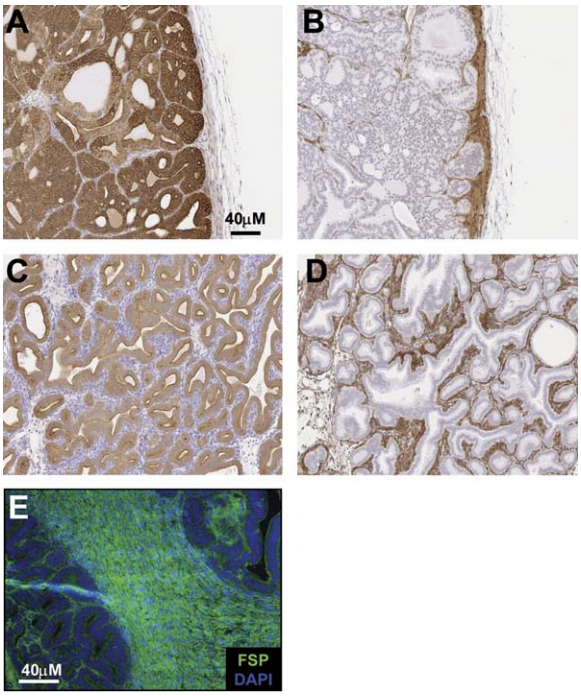

Figure 2. Marker Characterization of Stromal Tumors

Prostate lesions in *TgAPT*$_{121}$ mice at 12 weeks are comprised of aberrantly proliferating epithelial cells positive for cytokeratin 8 (brown, [A]) surrounded by smooth muscle actin (SMA)-positive mesenchyme (brown, [B]). The compartmental separation is retained within stromal tumors as demonstrated by the identical marker-staining profile: (C) cytokeratin 8, (D) SMA.

(A–D) Counterstained with hematoxylin. Expanding mesenchyme is also positive for fibroblast-specific protein marker S100A4 (FSP) by IF (E). Detection of FSP was with flourescein (green) and nuclei were counterstained with DAPI (blue).

expression by IF in prostates of all genotypes, early and after progression. In nontransgenic prostates, p53 was undetectable in both epithelium and stroma (Figure 4A). However, in the transgenic mice, where T_{121} was expressed specifically in the epithelium, the epithelial cells and a subset of mesenchymal cells expressed p53 (n = 10; Figure 4B), consistent with an induced p53 response in both compartments. It is currently unclear what the relevant p53 response(s) is (are) in epithelium, since neither apoptosis nor proliferation is affected by p53 deficiency (Hill et al., 2005). However, in the mesenchyme, p53 induction appears to suppress fibroblast proliferation, since these fibroblasts proliferate in a *p53*-deficient background (compare Figures 3 and 4). This mechanism was confirmed by the analysis of emerging stromal tumors in *TgAPT*$_{121}$;*p53*$^{+/-}$ prostates, where loss of p53 expression occurred specifically in the abundant stromal layers harboring proliferating fibroblasts while being retained in the epithelium (n = 18; Figures 4C and 4D). Loss of fibroblast p53 expression was not restricted to the *p53* heterozygous background, as mesenchyme from histologically identical tumors arising in *TgAPT*$_{121}$;*p53*$^{+/+}$ prostates had also undergone loss of p53 expression (n = 8; Figure 4E).

Stromal *p53* Mutation Selected during Tumor Progression

To determine whether loss of p53 expression could have resulted from the selection of fibroblasts that inactivated p53 by genetic mutation, stromal regions of *TgAPT*$_{121}$;*p53*$^{+/-}$ tumors were isolated by laser capture microdissection (LCM) and assayed by PCR for the presence of *p53* wild-type and null alleles (Figures 4F–4H). Strikingly, in four of six tumors analyzed, proliferating stroma had selectively lost the wild-type *p53* allele ($p < 0.0001$ by Binomial exact test; Figure 4H), while nonproliferative stromal regions associated with mPIN retained the wild-type *p53* allele (Figure 4H, *control stroma*). Moreover, when similar tumors arising in *TgAPT*$_{121}$;*p53*$^{+/+}$ prostates were analyzed for the number of *p53* gene copies present in the proliferative mesenchyme by quantitative PCR analyses, most had undergone allele reduction (Table 1). Of 11 LCM-stromal samples from 11 independent tumors, seven carried only a single *p53* copy while two had lost both copies. Two samples retained both *p53* copies. Statistical analysis showed loss of a single or both copies of *p53* to be highly significant ($p < 0.0001$) by the Binomial exact test. These data support the hypothesis that epithelial tumor initiation by cell cycle disruption places a strong selective pressure on the mesenchyme for loss of p53 function.

Notably, subsequent to p53 loss in the mesenchyme, some epithelial regions also lost p53 expression (Figures 5A–5C), further supporting an as-yet-unknown p53 tumor suppressor function in this compartment as well. Indeed, these tumors are heterogeneous, and many distinct neoplastic cell populations often coexist in the same gland. Epithelial cells that had lost p53 expression were morphologically similar to those of *TgAPT*$_{121}$;*p53*$^{-/-}$ prostate epithelium (Figure 1D) and produced lesions that were disorganized and pleiotropic compared to adjacent p53-positive epithelium (Figure 5A).

DISCUSSION

Our knowledge of genetic and epigenetic changes affecting cancer progression derives largely from analyses of events within the ''cancer cell'' itself. Indeed, animal-model studies show that cancer initiation and progression can be modeled by engineering specific lesions targeted to the presumed cell of origin (reviewed in Van Dyke and Jacks [2002]). However, sporadic human cancers evolve to harbor selective changes as a result of pressures imposed within a complex microenvironment. Each aberrant change can impact both the biology of the tumor cell and its surroundings (Hanahan and Weinberg, 2000), creating new selective pressures that likely affect the natural course of cancer evolution. Thus, full understanding requires experimental assessment of these evolutionary dynamics that ultimately produce a tumor with all the properties of a ''neoplastic organ.''

Recent reports have suggested the presence of tumor-suppressor mutations in the stroma of some human epithelial cancers (carcinomas), indicating that the selection of aberrant cells within the microenvironment occurs, likely

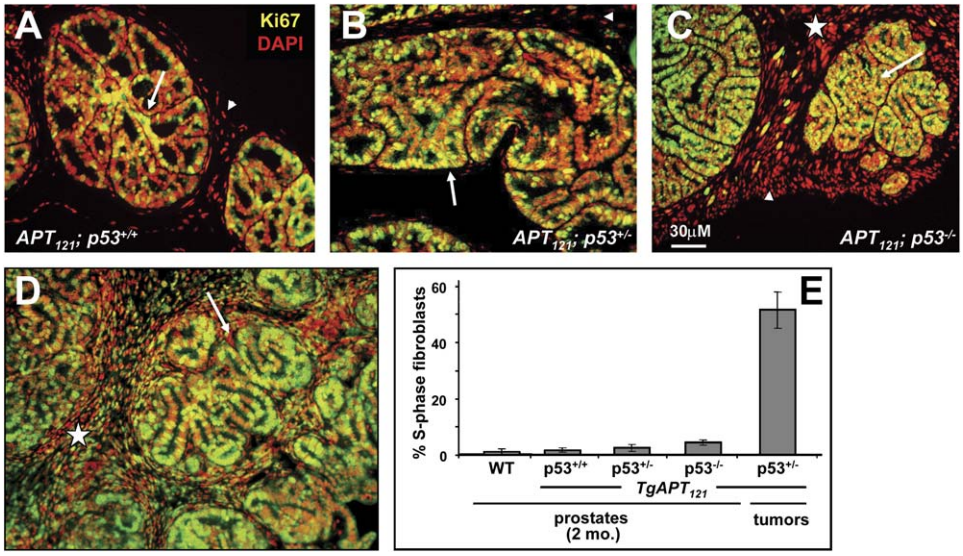

Figure 3. Proliferation Assessment in Subcompartments of Developing Tumors

Prostate samples were assessed for the expression of the S phase marker Ki67 via immunofluorescence in (A)–(D) (signal appears yellow as a merge of flourescein with red DAPI nuclear stain). The percentage of stromal cells positive for Ki67 were quantified in (E). Prostates of 2-month-old $TgAPT_{121};p53^{+/+}$ (A), $TgAPT_{121};p53^{+/-}$ (B), and $TgAPT_{121};p53^{-/-}$ mice (C) prior to tumor development show extensive proliferation in all epithelial compartments (arrows), while stromal (arrowheads) proliferation is only apparent in the hypercellular mesenchyme (star) of $TgAPT_{121};p53^{-/-}$ prostate (C and E). A significant increase in the proliferation index within the stroma occurs in tumors (E). A representative tumor with extensive stroma (star) from a 5-month-old $TgAPT_{121};p53^{+/-}$ mouse is shown in (D). In (E), the proliferation index is measured as the percentage of cells in S phase, calculated by counting Ki67-positive cells (yellow) as a percentage of total cells (DAPI red) of a given compartment based on morphology. Four random fields were examined for each tissue. Each data set was derived from analysis of 3 mice, and is expressed as mean ± SEM.

influencing cancer progression overall (Fukino et al., 2004; Kurose et al., 2001; Matsumoto et al., 2003; Moinfar et al., 2000; Paterson et al., 2003; Tuhkanen et al., 2004; Wernert et al., 2001). However, given the limitations of studying individual human samples and the inability to experimentally determine the role of putative microenvironment mutations during tumor progression, such reports have met with substantial skepticism. Here, through studies in mice genetically engineered to initiate prostate carcinoma (Hill et al., 2005), we show that cancer evolution can indeed involve the selection of genetic changes in the microenvironment as a result of nonautonomous pressures imposed by oncogenic stress within the epithelium.

Oncogenic Stress in Prostate Epithelium and a Tumor-Suppression Response in the Mesenchyme

To gain more insight into the role of p53 in prostate tumor suppression, we analyzed the development of prostate lesions in $TgAPT_{121}$ mice of *p53* heterozygous and nullizygous backgrounds. In $TgAPT_{121}$ mice, pRb function is absent in prostate epithelial cells due to cell-specific expression of T_{121}, a fragment of SV40 T antigen that binds and inactivates pRb, p107, and p130. As a result, the epithelial cells proliferate aberrantly triggering a cell-autonomous tumor-suppression response, the p53-independent induction of Pten-mediated apoptosis (Hill et al., 2005). The current genetic analysis of p53 function in this system led to the surprising discovery that this epithelial oncogenic stress also nonautonomously induces a p53 response in the associated prostate mesenchyme. In nontransgenic prostates, p53 is undetectable in both epithelium and stroma. However, in response to the inactivation of pRb function in the epithelium, p53 expression is induced in both the epithelial cells and in stromal fibroblasts consistent with a p53-dependent tumor-suppression response in both compartments. What the relevant response(s) is in epithelium is currently unknown, since neither apoptosis nor proliferation are quantitatively affected by p53 deficiency (Hill et al., 2005). However, in stromal fibroblasts, we show here that p53 plays a critical role in suppressing cell proliferation. When T_{121} is expressed in the prostate epithelium of *p53* null mice, associated stromal fibroblasts proliferate, resulting in an extensive hypercellular mesenchyme within 2 weeks of transgene induction.

Such an effect is not the result of p53 deficiency in the epithelium. In $TgAPT_{121};p53^{+/-}$ mice, loss of p53 expression in the mesenchyme during tumor progression is associated with fibroblast proliferation, while p53 expression is intact in the epithelium. Quantitative analysis of fibroblast proliferation shows proliferation in this compartment occurs only upon p53 inactivation and only in the presence of epithelial T_{121} expression. The fact that the proliferation rate of p53 null stromal fibroblasts soon after transgene induction is lower than that in tumors postselection suggests that only a subset of fibroblasts are initially responsive to the epithelial signal and then subsequently expand to constitute the major mesenchymal component of tumors. Thus, the data are consistent with a model in which oncogenic stress in the

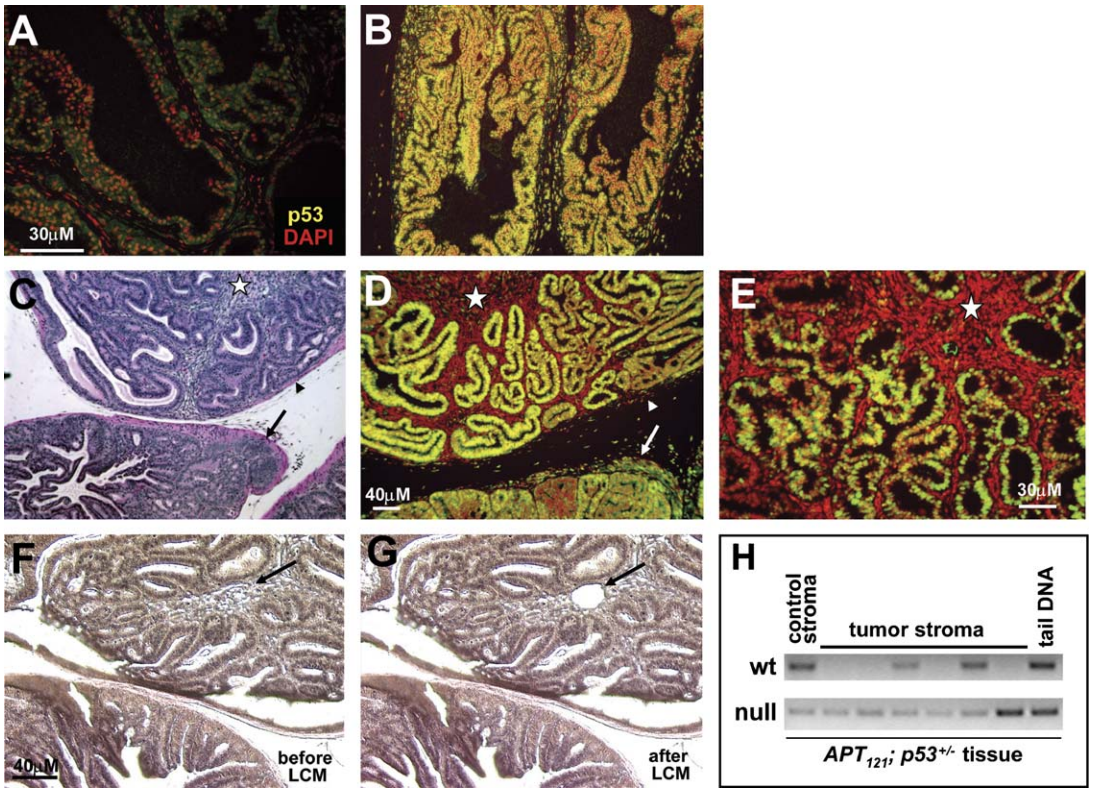

Figure 4. p53 Induction and Loss in *TgAPT$_{121}$;p53$^{+/-}$* Tumors

p53 expression was detected by IF (flourescein; yellow merge with DAPI red) in (A), (B), (D), and (E). At 2 months of age, p53 is undetectable in nontransgenic prostates (A) but significantly induced in both epithelial cells and stromal fibroblasts of *TgAPT$_{121}$* prostates (B). Serial sections of an emerging stromal tumor (arrowhead) with expanding mesenchyme (star) and adjacent mPIN (arrow) are shown in ([C]; H&E) and ([D]; p53 IF). p53 expression is lost in the tumor mesenchyme (star) and retained in the epithelium in addition to the mPIN-associated stroma (arrow). A total of 18 *TgAPT$_{121}$;+/p53$^{+/-}$* mice with stromal tumors were examined, and all were found to have lost p53 expression in the stroma. Similar stromal loss of p53 expression is observed in stromal tumors arising in *TgAPT$_{121}$;p53$^{+/+}$* mice (n = 8). A representative tumor from a 72-week-old mouse is shown in (E). An H&E-stained prostate section from a *TgAPT$_{121}$;p53$^{+/-}$* mouse is shown before (F) and after (G) laser-capture microdissection (arrow indicates the stromal region from which cells were isolated).

(H) PCR amplification specific for wild-type or null *p53* alleles was performed on laser-captured samples from *TgAPT$_{121}$;p53$^{+/-}$* mice, including control stroma (associated with dysplasia/PIN histology; e.g., [D], arrow) and stroma from six independent tumors. *TgAPT$_{121}$;p53$^{+/-}$* tail DNA served as a positive control. Binomial exact test showed loss of the wild-type *p53* allele in tumor stroma of *TgAPT$_{121}$;p53$^{+/-}$* mice was statistically significant ($p < 0.0001$).

epithelium provides a mitogenic signal to the mesenchyme, thus inducing a p53 response. p53 activation suppresses stromal fibroblast proliferation, constituting a selective pressure against p53 in that compartment (Figure 6).

Selective Evolution of the Mesenchyme Associated with Initiated Epithelium

To determine whether the highly proliferative stromal mesenchyme of tumors could have resulted from the selective expansion of fibroblasts that had undergone genetic inactivation of *p53*, stromal and epithelial regions of tumors were isolated by laser capture microdissection and assayed by PCR for the presence of *p53* wild-type and null alleles. Strikingly, proliferating stroma within the majority of tumors had indeed lost the wild-type *p53* allele, while nonproliferative stromal regions retained the wild-type *p53* allele. Importantly, similar mesenchymal *p53* loss occurred in ''sporadic'' stromal tumors arising at older ages in *TgAPT$_{121}$;p53$^{+/+}$* mice. The multicompartment evolution during *TgAPT$_{121}$* prostate tumor progression (Figure 6) indicates the likelihood that similar mechanisms are active during human tumorigenesis and may explain the stromal mutations previously observed in sporadic epithelial cancers.

For several reasons, it is unlikely that the stromal growth observed in these studies represents an EMT occurring after p53 loss. EMT is hypothesized to facilitate malignant tumor progression by causing the transdifferentiation of epithelial cells into a fibroblast-like phenotype (Thiery, 2002). However, from the earliest induction of T_{121} expression in the epithelium, p53 expression is induced in both the epithelial and mesenchymal compartments, while the boundaries between epithelial and stromal compartments are clearly preserved. Furthermore, germline inactivation of p53 together with T_{121} epithelial expression causes detectable proliferation of a subset of stromal fibroblasts. In all stages analyzed, including terminal tumors, there is no evidence of epithelial

Table 1. Loss of Wild-Type *p53* Alleles in Stromal Tumors of $TgAPT_{121}$ Mice

Tissue	Genotype	$2^{-\Delta\Delta Ct}$	Number of Wild-Type *p53* Alleles
Muscle	$p53^{+/+}$	1.473	2
Muscle	$p53^{+/+}$	0.679	2
Muscle	$p53^{+/-}$	0.524	1
Muscle	$p53^{+/-}$	0.593	1
Muscle	$p53^{-/-}$	0.112	0
Stromal tumor 1	$APT_{121};p53^{+/+}$	0.317	1
Stromal tumor 2	$APT_{121};p53^{+/+}$	0.567	1
Stromal tumor 3	$APT_{121};p53^{+/+}$	0.377	1
Stromal tumor 4	$APT_{121};p53^{+/+}$	0.579	1
Stromal tumor 5	$APT_{121};p53^{+/+}$	0.670	2
Stromal tumor 6	$APT_{121};p53^{+/+}$	0.398	1
Stromal tumor 7	$APT_{121};p53^{+/+}$	1.051	2
Stromal tumor 8	$APT_{121};p53^{+/+}$	0.035	0
Stromal tumor 9	$APT_{121};p53^{+/+}$	0.285	1
Stromal tumor 10	$APT_{121};p53^{+/+}$	0.046	0
Stromal tumor 11	$APT_{121};p53^{+/+}$	0.534	1

Real-time quantitative PCR was performed on DNA extracted from LCM samples to determine the status of wild-type *p53* alleles in stromal tumors or tissues of $TgAPT_{121}$ mice. LCM muscle samples were used as controls. Among 11 stromal tumor samples from 11 distinct animals, seven showed loss of one wild-type allele of *p53*, two showed loss of both alleles of *p53*, while two retained both wild-type alleles. $\Delta\Delta C_t$ = (sample C_t[*p53*] − sample C_t[β-*actin*]) − ($p53^{+/+}$ control Ct[*p53*] − $p53^{+/+}$ control C_t[β-*actin*]). C_t = the number of cycles required to reach a threshold value which is set within the exponential phase of the logarithmic scale amplification plot. Analysis of standard samples indicate that copy numbers of 2, 1, and 0 are indicated by $2^{-\Delta\Delta Ct}$ values of >0.6, between 0.15 to 0.6, and <0.15, respectively. Loss of a single and both copies of wild-type *p53* was statistically significant by Binomial exact test ($p < 0.0001$) assuming a random probability of 1%.

and fibroblast marker coexpression frequently observed in tumor-associated EMT (Saika et al., 2004). Additionally, the proliferative mesenchyme that develops in *p53* heterozygous, null, and wild-type backgrounds does not represent the selection of a normal p53 negative subpopulation but rather a selection for cells that have inactivated p53 by genetic loss. In contrast, loss of epithelial p53 expression is focally detectable significantly later (Figure 5).

Roles for Mutant Mesenchyme in Potentiating Epithelial Cancer

Analysis of the stromal tumors in $TgAPT_{121};p53^{+/-}$ prostates showed that loss of p53 expression occurred specifically in the stromal compartment while being retained in the epithelium. Interestingly, at later times, some regions of epithelium also lost p53 expression (Figure 5). Importantly, epithelial p53 loss was detectable only subsequent to mesenchymal p53 loss and expansion. This observation raises the possibility that p53-deficient stromal cells nonautonomously increase the selective pressure against p53 function in the epithelium. Epithelial regions with p53 loss were morphologically distinct from adjacent p53-expressing regions, including increased disorganization and nuclear atypia, as was apparent in *p53* null $TgAPT_{121}$ epithelium. Though currently correlative, this result suggests that a p53-deficient mesenchyme may also promote epithelial cell tumorigenesis by further altering the balance of selective pressures. In support of this hypothesis, a recent study showed that the tumorigenicity of MCF7 human breast cancer cells in SCID mice differed based on the host's *p53* status. Tumor onset occurred with reduced latency in p53-deficient recipients, indicating that p53-deficient stroma does indeed have the potential to accelerate epithelial tumorigenesis (Kiaris et al., 2005). Furthermore, the tumor stroma in *p53* heterozygous hosts showed *p53* LOH indicating the selection of p53-deficient fibroblasts is required (Kiaris et al., 2005). In our current studies, such changes occur during spontaneous tumor development subsequent to epithelial initiation.

Experimental tissue recombination studies in which epithelial and mesenchymal cells are isolated from normal or tumor samples, in some cases from distinct genotypes have demonstrated that the stromal compartment can effect neoplastic change within associated "normal" epithelium (Cunha et al., 2003). Recently, somatic interference with fibroblast TGF-β responsiveness via Cre-mediated inactivation of its receptor TBRII was shown to induce invasive squamous cell carcinoma of the forestomach and PIN in the prostate along with an increased abundance of stromal cells in these tissues (Bhowmick et al., 2004a). Thus, it is possible that selective changes in the stroma can lead to further selection of the epithelium. Whether such a mechanism explains the eventual loss of p53 and progression of the epithelium in $TgAPT_{121}$ prostate tumors is addressable by similar compartment-specific mutation or tissue-recombination approaches.

Implications for Human Cancers

Whether the model described here for p53 roles in mouse prostate tumorigenesis are directly relevant to mechanisms of human prostate cancer or can only be interpreted to reflect the possibility for multicompartment evolution in some epithelial tissues is not yet clear. In the $TgAPT_{121}$ model, p53 loss in fibroblasts associated with initiated epithelium results in the aggressive expansion of the mesenchyme, which ultimately comprises the bulk of the tumor, although slower-growing adenocarcinomas are clearly present. Whether the stromal overgrowth relative to carcinoma reflects mouse/human differences or is a property of the prostate remains to be determined. In the $TgAPT_{121}$ model, the spontaneous evolution of prostate epithelial tumor cells is extremely slow, progressing only to microinvasive adenocarcinoma (Hill et al., 2005). We previously showed that carcinoma progression is accelerated in a *Pten* heterozygous background, and progression of the carcinoma occurs spontaneously with

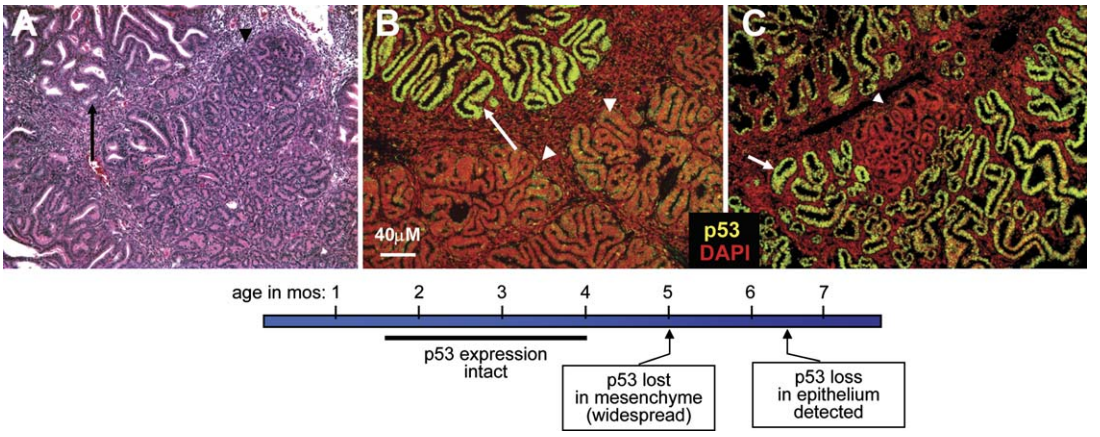

Figure 5. Epithelial p53 Loss Subsequent to Stromal p53 Loss Compounds Heterogeneous Tumor Progression

In H&E-stained $TgAPT_{121}$;$p53^{+/-}$ tumor sections (A), regions of dense epithelial cell growth morphologically distinct from surrounding epithelium (arrows) grow in small back-to-back circular glands (arrowheads). IF for p53 (yellow) shows that such regions no longer express p53 (B and C). Representative tumors from 7- (B) and 9 (C)-month-old $TgAPT_{121}$;$p53^{+/-}$ mice are shown. The blue bar indicates the relative timing of p53 expression and loss based on p53 IF analysis of prostates from $TgAPT_{121}$;$p53^{+/-}$ mice (n = 28). Focal epithelial loss occurred subsequent to p53 loss in the stroma.

Pten inactivation to invasive carcinoma (Hill et al., 2005). This result is consistent with the high incidence of Pten inactivation in advanced human prostate cancer (Feilotter et al., 1998; Ittmann, 1996). However, in a *Pten* wild-type background, such as in the present study, spontaneous Pten loss and carcinoma progression has not been observed, possibly reflecting a species-specific constraint on allele loss. The resistance to spontaneous epithelial Pten inactivation may explain dominance of the proliferative mesenchyme upon selective p53 loss. It is interesting that Li-Fraumeni patients have a low incidence of prostate cancer (Kleihues et al., 1997), although they do display a higher-than-normal incidence of phylloides cancers (Birch et al., 2001). Also, rare human malignant phylloides cancers in the prostate and breast lack p53 expression in both epithelial and stromal cell components (McCarthy et al., 2004) or express mutant p53 (Gatalica et al., 2001).

The present studies do provide evidence that coevolution of the stromal compartment, with selection of genetically altered cells, can occur as a result of oncogenic stress in the epithelium. Such mechanisms may explain the observation of stromal tumor-suppressor mutations, including in *p53* (Kurose et al., 2002; Paterson et al., 2003) and in *Pten* (Kurose et al., 2002), in human carcinomas, including breast (Fukino et al., 2004; Kurose et al., 2001; Moinfar et al., 2000; Wernert et al., 2001), colon (Matsumoto et al., 2003; Wernert et al., 2001), and ovary (Tuhkanen et al., 2004). Our work represents the first in vivo model of spontaneous tumor progression to identify selective mutation in reactive stroma as a mechanism for neoplastic acceleration, suggesting

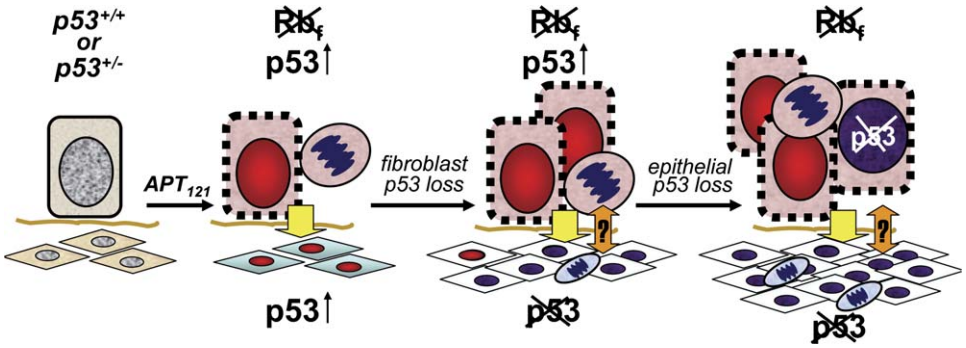

Figure 6. A Model for Multicompartment Tumor Evolution Triggered by Epithelial Cell Disruption

Normal epithelial-mesenchymal interactions are perturbed by cell cycle disruption (depicted as a mitotic figure) in the epithelium upon inactivation of pRb, p107, and p130 (dashed black border). As a result, p53 is induced in both epithelial cells and stromal fibroblasts (red nuclei). Non-cell-autonomous signals from initiated epithelium induce a p53 growth-suppression response in stromal fibroblasts (yellow arrow), which creates selective pressure against p53 function. Once p53 is inactivated (navy nuclei), stromal fibroblasts proliferate in continued response to the aberrant epithelium. p53 expression is subsequently lost in some epithelial cells, either stochastically or by generation of new selective pressures conferred by aberrant stroma (orange arrow). This model is consistent with the full body of data presented herein.

that stromal mutation in epithelial cancer can play a significant role in overall cancer development. These studies underscore the dynamic complexity of cell-cell interactions and the changing selective microenvironment that drives cancer development. Whether cells in the microenvironment in addition to fibroblasts are susceptible to selective genetic change remains to be determined. However, the present results encourage further exploration of this possibility and emphasize both the need to determine the cell of origin for mutations detected in human cancers and the potential importance for developing cancer therapies that target the stromal compartment as a means to prevent acceleration or possibly even suppress tumorigenesis.

EXPERIMENTAL PROCEDURES

Breeding Strategies

Derivation of *TgAPT$_{121}$* transgenic mice was previously described (Hill et al., 2005). *TgAPT$_{121}$* mice were identified by PCR amplification of a 160 bp T_{121} fragment using primers 5′-GAATCTTTGCAGCTAATGGACC-3′ and 5′-GCATCCCAGAAGCTCCAAAG-3′ and digit-derived genomic DNA as template. The cycling profile was as follows: 94ºC, 2 min; 35 cycles of 94ºC, 20 s; 62ºC, 45 s; 72ºC, 45 s; and final incubation at 72ºC, 2 min. *TgAPT$_{121}$* mice were maintained by crossing to nontransgenic B6D2F1 mice and therefore are designated as B6; D2-TgAPT$_{121}$ (Tvd *TgAPT$_{121}$*). To study the effect of *p53* inactivation on prostate tumorigenesis, *TgAPT$_{121}$* mice were mated to *p53* nullizygous mice (p53tm1Tyj; Jackson Laboratory). *p53* genotypes were determined by PCR using two reactions (Lowe et al., 1993): one amplifies the neomycin insertion site (neomycin primer, 5′-TCCTCGTGCTTTACGGTATC-3′; *p53* primer, 5′-TATACTCAGAGCCGGCCT-3′; 525 bp product) and the other amplifies the endogenous *p53* allele (substituting 5′-ACAGCGTGGTGGTACCTTAT-3′ for the neomycin primer, 475 bp product). Cycling parameters were the same as for the T_{121} reaction described above. We used standard breeding strategies to produce *TgAPT$_{121}$;p53$^{+/+}$*, *TgAPT$_{121}$;p53$^{+/-}$*, and *TgAPT$_{121}$;p53$^{-/-}$* mice, and nontransgenic male littermates (*p53$^{+/+}$*, *p53$^{+/-}$*, or *p53$^{-/-}$*) served as controls.

Histopathology

Prostate and tumor samples were dissected from male mice, and a portion was fixed overnight in 10% phosphate-buffered formalin, transferred to 70% ethanol, then embedded in paraffin. To analyze tumor morphology and development, prostate samples were sectioned for 10 successive layers at 5 μm intervals and stained with hematoxylin and eosin (H&E) for histopathological examination as previously described (Hill et al., 2005).

Immunodetection

Immunohistochemical analysis was performed on formalin-fixed paraffin sections. Antigen retrieval for all antibodies was by boiling in citrate buffer (pH 6.0; Zymed, South San Francisco, CA) for 15 min. Endogenous peroxidase activity was quenched with a 10 min incubation in 3% H_2O_2 in methanol. Antibodies used were anti-cytokeratin 8 (1:100, sheep polyclonal, PH182, Binding Site, Birmingham, UK), anti-smooth muscle actin (1:1000, mouse A2537, Sigma, St. Louis, MO), anti-p53 (1:500, rabbit polyclonal CM5, Novocastra, Newcastle upon Tyne, NE12 8EW, UK), anti-SV40 T antigen (N-terminal-specific monoclonal Ab2, 1:100, Oncogene, Cambridge, MA), anti-Ki67 (1:2000, goat polyclonal M-19, Santa Cruz Biotechnology, Santa Cruz, CA), and anti-FSP (S100A4) (1:500, mouse 1B10, Sigma, St. Louis, MO). Detection for all antibodies was performed using the Vector ABC Elite Kit and a Vector DAB kit for substrate detection (Vector Labs, Burlingame, CA). Immunofluorescence followed the same protocols except that signal amplification used the TSA Plus Fluorescence System (Perkin Elmer, Wellesley, MA). Slides were counterstained with DAPI and mounted using Vector Hardset Mounting Media (Vector Labs, Burlingame, CA).

Laser-Capture Microdissection and LOH Analysis

Laser-capture microdissection (LCM) of H&E-stained sections was performed using a Leica AS LMD with a pulsed 337 nm UV laser (Leica Microsystems Inc., Bannockburn, IL). Formalin-fixed paraffin-embedded tissue sections were mounted onto Glass Foiled PEN slides (Vashaw Scientific, Atlanta, GA). Cells were collected in a cap of the tube containing 50 μl of lysis buffer (10 mM Tris-HCl [pH 8.0], 1% Tween 20). Following specimen collection, the samples were spun for 15 s and then 5 μl of proteinase K (100 mg/ml) was added to the samples, which were incubated at 55ºC overnight. Proteinase K was inactivated at 99ºC for 10 min, and 5–10 μl aliquots were used for PCR analysis. The primers for semiquantitative PCR were as follows: wild-type *p53* (173 bp) forward 5′-CATCACCTCACTGCATGGAC-3′, reverse 5′-AAAAGATGACAGGGGCCATG-3′; *Neo* (*p53 null*; 160 bp) forward 5′-ATGATTGAACAAGATGGATTGC-3′, reverse 5′-ACAGGTCGGTCTTGACAAAA-3′. The PCR condition was 94ºC 10 min, 35 cycles of 94ºC 30 s, 58ºC 90 s, and 72ºC 45 s, and 72ºC 10 min. Products were resolved in 2% agarose gels and visualized under UV light. Quantitative real-time PCR analysis was performed on LCM TgAPT$_{121}$;p53$^{+/+}$ stromal tumors and tissue samples to determine the status of wild-type *p53* alleles. Primers were as follows: *p53* forward (FAM labeled) 5′-caacagaCTCACTGCATGGACGATCTGtTG-3′, reverse 5′-GGCTTCACTTGGGCCTTCAA-3′; β-*actin* forward 5′-GGTGGGAATGGGTCAGAAGG-3′, reverse (Joe labeled) 5′-caactgTCTCCATGTCGTCCCAGtTG-3′ (Invitrogen Life Technologies, Carlsbad, CA). Each 12 μl reaction mixture contained 5 μl of LCM DNA template, 200 nM p53 primers, 200 nM β-actin primers, 200 nM deoxynucleoside triphosphates, 1.2 μl of 10× buffer, and 0.3 U Taq DNA polymerase (Boehringer Mannheim, Germany). Cycling was as follows: 94ºC 2 min, 40 cycles of 94ºC 15 s, 58ºC 30 s, and 72ºC 60 s. The reaction was performed in 384-well clear optical reaction plate (Applied Biosystems, Foster City, CA) using ABI7700 Sequence Detection System (Applied Biosystems, Foster City, CA), and the data were analyzed using SDS 2.1 software (Applied Biosystems, Foster City, CA) and standard protocols (http://www.appliedbiosystems.com). The copy number of each sample was determined by calculating $\Delta\Delta C_t$ based on the formula $\Delta\Delta C_t$ = (sample C_t[p53] − sample C_t[β-*actin*]) − (*p53$^{+/+}$* control C_t[p53] − *p53$^{+/+}$* control C_t[β-*actin*]), where C_t is the number of cycles required to reach a threshold based on linear amplification. The *p53$^{+/+}$* control C_t for *p53* and β-*actin* was the average C_t of the two *p53$^{+/+}$* muscle samples. Analyses of standard samples indicate copy numbers of 2, 1, and 0 by $2^{-\Delta\Delta Ct}$ values of >0.6, 0.15 to 0.6, and <0.15, respectively.

Statistical Analysis

A Binomial exact test was performed using SAS 9.1 (Cary, NC) to determine whether loss of the wild-type *p53* allele was statistically significant in tumor stroma of *TgAPT$_{121}$;p53$^{+/-}$* and *TgAPT$_{121}$;p53$^{+/+}$* mice. The probability of random wild-type *p*53 allele loss in the tumor stroma was arbitrarily set at 1%. However, results remain significant ($p < 0.0001$) even if the probability of random loss is as high as 10%.

ACKNOWLEDGMENTS

We thank Huoy Lim, Shannon Meyer for expert technical assistance, the UNC histopathology core facility for processing slides, Michael Hooker Microscopy core facility for LCM experiments, and the UNC Division of Laboratory Animal Medicine for excellent animal care. We also thank the members of the Van Dyke Lab for many insightful discussions. This work was supported by a grant from the National Cancer Institute to T.V.D. (R01-CA046283) and to R.D.C. (U01-CA84294).

Received: August 10, 2005
Revised: September 6, 2005
Accepted: September 20, 2005
Published: December 15, 2005

REFERENCES

Barcellos-Hoff, M.H., and Ravani, S.A. (2000). Irradiated mammary gland stroma promotes the expression of tumorigenic potential by unirradiated epithelial cells. Cancer Res. *60*, 1254–1260.

Bergers, G., and Coussens, L.M. (2000). Extrinsic regulators of epithelial tumor progression: metalloproteinases. Curr. Opin. Genet. Dev. *10*, 120–127.

Bhowmick, N.A., Chytil, A., Plieth, D., Gorska, A.E., Dumont, N., Shappell, S., Washington, M.K., Neilson, E.G., and Moses, H.L. (2004a). TGF-beta signaling in fibroblasts modulates the oncogenic potential of adjacent epithelia. Science *303*, 848–851.

Bhowmick, N.A., Neilson, E.G., and Moses, H.L. (2004b). Stromal fibroblasts in cancer initiation and progression. Nature *432*, 332–337.

Birch, J.M., Alston, R.D., McNally, R.J., Evans, D.G., Kelsey, A.M., Harris, M., Eden, O.B., and Varley, J.M. (2001). Relative frequency and morphology of cancers in carriers of germline TP53 mutations. Oncogene *20*, 4621–4628.

Cunha, G.R., Reese, B.A., and Sekkingstad, M. (1980). Induction of nuclear androgen-binding sites in epithelium of the embryonic urinary bladder by mesenchyme of the urogenital sinus of embryonic mice. Endocrinology *107*, 1767–1770.

Cunha, G.R., Hayward, S.W., Dahiya, R., and Foster, B.A. (1996). Smooth muscle-epithelial interactions in normal and neoplastic prostatic development. Acta Anat. (Basel) *155*, 63–72.

Cunha, G.R., Hayward, S.W., Wang, Y.Z., and Ricke, W.A. (2003). Role of the stromal microenvironment in carcinogenesis of the prostate. Int. J. Cancer *107*, 1–10.

Dameron, K.M., Volpert, O.V., Tainsky, M.A., and Bouck, N. (1994). The p53 tumor suppressor gene inhibits angiogenesis by stimulating the production of thrombospondin. Cold Spring Harb. Symp. Quant. Biol. *59*, 483–489.

Dannenberg, J.H., van Rossum, A., Schuijff, L., and te Riele, H. (2000). Ablation of the retinoblastoma gene family deregulates G(1) control causing immortalization and increased cell turnover under growth-restricting conditions. Genes Dev. *14*, 3051–3064.

Feilotter, H.E., Nagai, M.A., Boag, A.H., Eng, C., and Mulligan, L.M. (1998). Analysis of PTEN and the 10q23 region in primary prostate carcinomas. Oncogene *16*, 1743–1748.

Fukino, K., Shen, L., Matsumoto, S., Morrison, C.D., Mutter, G.L., and Eng, C. (2004). Combined total genome loss of heterozygosity scan of breast cancer stroma and epithelium reveals multiplicity of stromal targets. Cancer Res. *64*, 7231–7236.

Gatalica, Z., Finkelstein, S., Lucio, E., Tawfik, O., Palazzo, J., Hightower, B., and Eyzaguirre, E. (2001). p53 protein expression and gene mutation in phyllodes tumors of the breast. Pathol. Res. Pract. *197*, 183–187.

Hanahan, D., and Weinberg, R.A. (2000). The hallmarks of cancer. Cell *100*, 57–70.

Harris, S.L., and Levine, A.J. (2005). The p53 pathway: positive and negative feedback loops. Oncogene *24*, 2899–2908.

Hill, R., Song, Y., Carrdiff, R.D., and Van Dyke, T. (2005). Heterogeneous tumor evolution initiated by loss of pRb function in a preclinical prostate cancer model. Cancer Res. *65*, 10243–10254.

Hollstein, M., Sidransky, D., Vogelstein, B., and Harris, C.C. (1991). p53 mutations in human cancers. Science *253*, 49–53.

Ittmann, M. (1996). Allelic loss on chromosome 10 in prostate adenocarcinoma. Cancer Res. *56*, 2143–2147.

Johnson, R.L., and Tabin, C.J. (1997). Molecular models for vertebrate limb development. Cell *90*, 979–990.

Kiaris, H., Chatzistamou, I., Trimis, G., Frangou-Plemmenou, M., Pafiti-Kondi, A., and Kalofoutis, A. (2005). Evidence for nonautonomous effect of p53 tumor suppressor in carcinogenesis. Cancer Res. *65*, 1627–1630.

Kleihues, P., Schauble, B., zur Hausen, A., Esteve, J., and Ohgaki, H. (1997). Tumors associated with p53 germline mutations: a synopsis of 91 families. Am. J. Pathol. *150*, 1–13.

Kurose, K., Hoshaw-Woodard, S., Adeyinka, A., Lemeshow, S., Watson, P.H., and Eng, C. (2001). Genetic model of multi-step breast carcinogenesis involving the epithelium and stroma: clues to tumour-microenvironment interactions. Hum. Mol. Genet. *10*, 1907–1913.

Kurose, K., Gilley, K., Matsumoto, S., Watson, P.H., Zhou, X.P., and Eng, C. (2002). Frequent somatic mutations in PTEN and TP53 are mutually exclusive in the stroma of breast carcinomas. Nat. Genet. *32*, 355–357.

Lee, M.H., Williams, B.O., Mulligan, G., Mukai, S., Bronson, R.T., Dyson, N., Harlow, E., and Jacks, T. (1996). Targeted disruption of p107: functional overlap between p107 and Rb. Genes Dev. *10*, 1621–1632.

Levine, A.J., Momand, J., and Finlay, C.A. (1991). The p53 tumour suppressor gene. Nature *351*, 453–456.

Lowe, S.W., Schmitt, E.M., Smith, S.W., Osborne, B.A., and Jacks, T. (1993). p53 is required for radiation-induced apoptosis in mouse thymocytes. Nature *362*, 847–849.

Luo, R.X., Postigo, A.A., and Dean, D.C. (1998). Rb interacts with histone deacetylase to repress transcription. Cell *92*, 463–473.

Matsumoto, N., Yoshida, T., Yamashita, K., Numata, Y., and Okayasu, I. (2003). Possible alternative carcinogenesis pathway featuring microsatellite instability in colorectal cancer stroma. Br. J. Cancer *89*, 707–712.

McCarthy, R.P., Zhang, S., Bostwick, D.G., Qian, J., Eble, J.N., Wang, M., Lin, H., and Cheng, L. (2004). Molecular genetic evidence for different clonal origins of epithelial and stromal components of phyllodes tumor of the prostate. Am. J. Pathol. *165*, 1395–1400.

Mericskay, M., Kitajewski, J., and Sassoon, D. (2004). Wnt5a is required for proper epithelial-mesenchymal interactions in the uterus. Development *131*, 2061–2072.

Moinfar, F., Man, Y.G., Arnould, L., Bratthauer, G.L., Ratschek, M., and Tavassoli, F.A. (2000). Concurrent and independent genetic alterations in the stromal and epithelial cells of mammary carcinoma: implications for tumorigenesis. Cancer Res. *60*, 2562–2566.

Nigro, J.M., Baker, S.J., Preisinger, A.C., Jessup, J.M., Hostetter, R., Cleary, K., Bigner, S.H., Davidson, N., Baylin, S., Devilee, P., et al. (1989). Mutations in the p53 gene occur in diverse human tumour types. Nature *342*, 705–708.

Ohuchida, K., Mizumoto, K., Murakami, M., Qian, L.W., Sato, N., Nagai, E., Matsumoto, K., Nakamura, T., and Tanaka, M. (2004). Radiation to stromal fibroblasts increases invasiveness of pancreatic cancer cells through tumor-stromal interactions. Cancer Res. *64*, 3215–3222.

Paterson, R.F., Ulbright, T.M., MacLennan, G.T., Zhang, S., Pan, C.X., Sweeney, C.J., Moore, C.R., Foster, R.S., Koch, M.O., Eble, J.N., and Cheng, L. (2003). Molecular genetic alterations in the laser-capture-microdissected stroma adjacent to bladder carcinoma. Cancer *98*, 1830–1836.

Podlasek, C.A., Barnett, D.H., Clemens, J.Q., Bak, P.M., and Bushman, W. (1999). Prostate development requires Sonic hedgehog expressed by the urogenital sinus epithelium. Dev. Biol. *209*, 28–39.

Robanus-Maandag, E., Dekker, M., van der Valk, M., Carrozza, M.L., Jeanny, J.C., Dannenberg, J.H., Berns, A., and te Riele, H. (1998). p107 is a suppressor of retinoblastoma development in pRb-deficient mice. Genes Dev. *12*, 1599–1609.

Sage, J., Mulligan, G.J., Attardi, L.D., Miller, A., Chen, S., Williams, B., Theodorou, E., and Jacks, T. (2000). Targeted disruption of the three Rb-related genes leads to loss of G(1) control and immortalization. Genes Dev. *14*, 3037–3050.

Saika, S., Kono-Saika, S., Ohnishi, Y., Sato, M., Muragaki, Y., Ooshima, A., Flanders, K.C., Yoo, J., Anzano, M., Liu, C.Y., et al. (2004). Smad3 signaling is required for epithelial-mesenchymal transition of lens epithelium after injury. Am. J. Pathol. *164*, 651–663.

Sakakura, T. (1991). New aspects of stroma-parenchyma relations in mammary gland differentiation. Int. Rev. Cytol. *125*, 165–202.

Shappell, S.B., Thomas, G.V., Roberts, R.L., Herbert, R., Ittmann, M.M., Rubin, M.A., Humphrey, P.A., Sundberg, J.P., Rozengurt, N., Barrios, R., et al. (2004). Prostate pathology of genetically engineered mice: definitions and classification. The consensus report from the Bar Harbor meeting of the Mouse Models of Human Cancer Consortium Prostate Pathology Committee. Cancer Res. *64*, 2270–2305.

Strutz, F., Okada, H., Lo, C.W., Danoff, T., Carone, R.L., Tomaszewski, J.E., and Neilson, E.G. (1995). Identification and characterization of a fibroblast marker: FSP1. J. Cell Biol. *130*, 393–405.

Thiery, J.P. (2002). Epithelial-mesenchymal transitions in tumour progression. Nat. Rev. Cancer *2*, 442–454.

Tlsty, T.D., and Hein, P.W. (2001). Know thy neighbor: stromal cells can contribute oncogenic signals. Curr. Opin. Genet. Dev. *11*, 54–59.

Tuhkanen, H., Anttila, M., Kosma, V.M., Yla-Herttuala, S., Heinonen, S., Kuronen, A., Juhola, M., Tammi, R., Tammi, M., and Mannermaa, A. (2004). Genetic alterations in the peritumoral stromal cells of malignant and borderline epithelial ovarian tumors as indicated by allelic imbalance on chromosome 3p. Int. J. Cancer *109*, 247–252.

Van Dyke, T., and Jacks, T. (2002). Cancer modeling in the modern era: Progress and challenges. Cell *108*, 135–144.

Vousden, K.H. (2002). Activation of the p53 tumor suppressor protein. Biochim. Biophys. Acta *1602*, 47–59.

Vousden, K.H., and Lu, X. (2002). Live or let die: the cell's response to p53. Nat. Rev. Cancer *2*, 594–604.

Wernert, N., Locherbach, C., Wellmann, A., Behrens, P., and Hugel, A. (2001). Presence of genetic alterations in microdissected stroma of human colon and breast cancers. Anticancer Res. *21*, 2259–2264.

Xiao, A., Wu, H., Pandolfi, P.P., Louis, D.N., and Van Dyke, T. (2002). Astrocyte inactivation of the pRb pathway predisposes mice to malignant astrocytoma development that is accelerated by PTEN mutation. Cancer Cell *1*, 157–168.

Yu, E.Y., Yu, E., Meyer, G.E., and Brawer, M.K. (1997). The relation of p53 protein nuclear accumulation and angiogenesis in human prostatic carcinoma. Prostate Cancer Prostatic Dis. *1*, 39–44.